ACS Catalysis

RESEARCH ARTICLE

pubs.acs.org/acscatalysis

Role of Cs on Hydrodesulfurization Activity of RuS_2 Catalysts Supported on a Mesoporous SBA-15 Type Material

A. Infantes-Molina,*[,†] A. Romero-Pérez,[‡] V. Sánchez-González,[‡] B. Pawelec,[†] J. L.G. Fierro,[†] A. Jiménez-López,[‡] and E. Rodríguez-Castellón*[,‡]

[†]Instituto de Catálisis y Petroleoquímica, CSIC, Cantoblanco, 28049 Madrid, Spain

[‡]Departamento de Química Inorgánica, Crystalografía y Mineralogía (Unidad Asociada al ICP-CSIC), Facultad de Ciencias, Universidad de Málaga, Campus de Teatinos, 29071 Málaga, Spain

ABSTRACT: RuS_2-Cs catalysts supported on SBA-15 type mesoporous materials for hydrodesulfurization (HDS) of dibenzothiophene (DBT) were synthesized. The influence of cesium content and sulfiding temperature (500 and 600 °C), as well as the cesium precursor salt employed (cesium hydroxide and cesium chloride), was studied. The quantity of ruthenium was maintained constant while the amount of cesium variable, with Cs/Ru molar ratios of 0.1:1, 0.5:1, and 1:1. The support, precursors, sulfided, and spent catalysts were characterized by X-ray diffraction (XRD), N_2 adsorption−desorption isotherms at −196 °C, transmission electron microscopy (TEM), X-ray photoelectron spectroscopy (XPS) analysis, H_2-TPRS, TPO, and DRIFT spectra of adsorbed NO. The catalytic properties of these materials were tested between 260 and 440 °C in the HDS of DBT under a hydrogen pressure of 3.0 MPa. The obtained results reveal that in mesoporous materials, the presence of cesium induces the agglomeration of the RuS_2 active phase, that is, the lower the cesium content the better the RuS_2 dispersion. In this sense, the catalysts with the lowest amount of Cs present the best catalytic results and at lower reaction temperatures. In terms of selectivity, the presence of Cs leads the DBT HDS reaction toward the direct desulfurization route (DDS) with a selectivity to biphenyl (BP) close to 100%. The cesium precursor salt employed did not modify the dispersion of Ru phase in the Cs-Ru/SBA-15 catalysts but affected the sulfur lability of the catalyst.

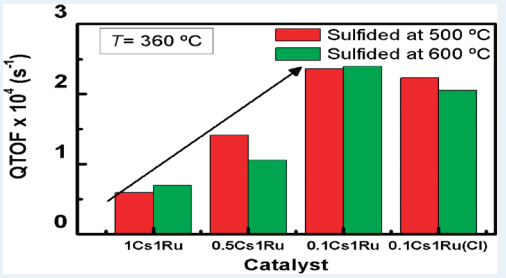

KEYWORDS: mesoporous SBA-15, cesium, ruthenium sulfide, dibenzothiophene, HDS

1. INTRODUCTION

At the moment, the environmental and governmental laws are more and more strict to decrease the sulfur quantity in diesel fuel up to 15 ppm for the U.S.A.[1] and 10 ppm for E.U.[2] For this reason, nowadays, researchers in this area are seeking better catalysts to achieve such goals. In general, a catalyst must have basic features such as high efficiency, activity, and stability, as well as a great selectivity; nonetheless, those characteristics are challenging to achieve. The transition metal sulfides (TMS) have been widely studied because of their noteworthy catalytic properties for hydrotreating reactions. Pecoraro and Chianelli[3] reported the great catalytic activity for bulk transition metals sulfides (TMS); since this milestone work, there have been important findings to obtain alternative catalysts, specially, for hydrodesulfurization (HDS), hydrodenitrogenation (HDN), and hydrogenation (HYD) reactions. Such metals were plotted into a curve called "volcano plot" where the HDS activity per mole of metal versus the M−S bond strength was plotted.[4] It was observed that the first TMS row is relatively inactive, but the second and third TMS rows exhibit a maximum in activity, the RuS_2 phase being the most active.[3]

Unsupported RuS_2 appeared to be 13 times more active than MoS_2 in HDS,[3] and the supported RuS_2 has been also extensively studied (ref 5 and references therein). However, there is a large discrepancy concerning the supported RuS_2 on different materials, which is due to the different precursors, activation procedures, and supports employed for this purpose.[5−9] Ruthenium has been also employed as promoter of Ni and Mo systems[10−12] or as second promoter of NiMoS catalysts.[13−15] In general, promising catalytic activities have been obtained when using ternary compounds containing Ru. In this sense, it was reported that the incorporation of ruthenium on NiMo sulfided catalysts using several supports, for HDN, HDS, and hydrodearomatization (HDA) reactions, provoked an enhancement of their catalytic activity.[14]

It is well-known that bulk ruthenium sulfide presents an uppermost catalytic activity in HDS reactions.[3] Raje et al.[16] studied the removal of individual sulfur compounds of a coal-derived naphtha with several bulk TMS. They found that ruthenium and rhodium were the most active with total sulfur removal levels greater than 90%. Moreover, in a simultaneous removal of sulfur, nitrogen, and oxygen compounds from a coal-derived naphtha, RuS_2

Received: October 17, 2010
Revised: January 14, 2011
Published: February 03, 2011

presented the highest activity for all three of the hydrotreating processes.[17] However, when the RuS_2 phase is supported, the results found in the literature are diverse. On one hand a lower activity was observed because of its reduction into metallic ruthenium under the reducing conditions employed in the catalytic test,[7] and if it is supported on alumina, sulfiding temperatures higher than 500 °C are required to form the RuS_2 phase with pyrite-like structure, which is the true active phase for hydrotreating reactions. On the other hand, it has been reported that Ru/γ-Al_2O_3 catalyst sulfided in 100% H_2S at 400 °C possessed about 7-fold higher thiophene conversion rates than CoMo/γ-Al_2O_3 when compared per square meter of active area.[8] Moreover RuS_2 supported on a Y-zeolite was reported to have a higher HDS activity than supported on γ-Al_2O_3.[9] As perfectly described by Quartararo et al.,[18] there are many factors during the synthesis of ruthenium sulfide catalysts that must be taken into account for controlling their physicochemical properties, and as a consequence for achieving a good performance with this kind of catalysts. It is recommended no calcination after the incorporation of ruthenium chloride and the sulfiding mixture should be H_2S/N_2 to achieve a high degree of sulfurization and to avoid the reduction of the RuS_2 phase formed (ref 5 and references therein). Furthermore, the sulfiding temperature influences the catalytic behavior[19] as well as the crystallographic orientations that induce the preference toward HDS and HYD reactions.

Ishihara et al.[20] were the first to report the addition of alkali metals to RuS_2 catalysts supported on Al_2O_3. The addition of NaOH did not improve the HDS reaction because of the poisoning of some sites. Nonetheless, a cesium-promoted Ru catalyst with a Ru/Cs molar ratio of 1:2 exhibited HDS activities comparable to that of a conventional Co−Mo catalyst.[21] The insertion of atoms like cesium seems to enhance the number of labile sulfur, aids to stabilize the RuS_2 active phase as it strengths Ru−S bond of ruthenium sulfide, and promotes the C−S bond scission of DBT, and therefore the catalytic activity increases.[22,23] However, if a Cs excess is present, the formation of H_2S and regeneration of coodinatively unsaturated sites are prevented, which results in a decrease in the catalytic activity.

In a previous work, a family of RuS_2 catalysts supported on SBA-15 type mesoporous silica, and that doped with zirconium and aluminum, were prepared and tested in the HDS of DBT.[24] The catalysts turned out to be highly active and stable. Considering the important role of cesium on RuS_2 type catalysts reported in the literature, and the favorable characteristics of SBA-15 type material to obtain highly dispersed RuS_2 particles, it has been considered interesting to evaluate the addition of cesium to a mesoporous support to prepare RuS_2 active catalysts.

2. EXPERIMENTAL SECTION

2.1. Materials. The support used in this study was a SBA-15 mesoporous silica (Si-SBA). Ruthenium(III) chloride, $RuCl_3 \cdot n$-H_2O (~ 41 wt % Ru, from Fluka); cesium hydroxide, CsOH (50 wt % solution, from Aldrich); and cesium chloride, CsCl (99.9% from Aldrich) were employed as ruthenium and cesium precursor salts, respectively. The chemical products utilized in the reactivity study were dibenzothiophene (Aldrich 98%) in *cis*-, *trans*-decahydronaphthalene (Sigma-Aldrich 98%). The gases employed were H_2S/N_2 10/90% (Air liquide 99.99%), He (Air Liquide 99.99%), H_2 (Air Liquide 99.999%), and N_2 (Air Liquide 99.9999%).

Table 1. Nominal Composition* and Textural Properties of the Samples

sample	Ru (wt %)*	Cs (wt %)*	S_{BET} (m^2g^{-1})	V_p ($cm^3\ g^{-1}$)[a]	d_p (nm)[b]
Support					
Si-SBA			635	0.55	4.0
Sulfided Catalysts					
1Cs1RuSiS500	6.4	8.4	93	0.12	3.5
1Cs1RuSiS600			82	0.11	3.5
0.5Cs1RuSiS500	6.7	4.4	83	0.13	3.9
0.5Cs1RuSiS600			52	0.10	3.7
0.1Cs1RuSiS500	6.9	0.9	293	0.29	3.6
0.1Cs1RuSiS500 (Cl)	6.9	0.9	319	0.30	3.6

[a] V_p Calculated at $P/P_0 = 0.95$ [b] d_p BJH method to the desorption branch

2.2. Preparation of Catalysts. SBA-15 mesoporous silica (Si-SBA) prepared using a low cost method[25] was used as a support. Thus, in a typical synthesis, 5 g of template, Triblock copolymer Pluronic P123, was dissolved in 200 mL of 0.4 M H_2SO_4 solution. After stirring for a few hours, a clear solution was obtained. Then, 0.2 g of NaOH and 13.3 mL of sodium silicate solution were added at room temperature under stirring. The resulting gel mixture was stirred for 5 days at room temperature. The solid product was recovered by filtration, washed several times with deionized water and dried overnight at 60 °C. Finally, the material was calcined at 550 °C for 6 h (heating rate 10 °C min^{-1}).

A family of ruthenium sulfided catalysts doped with cesium and supported on Si-SBA was prepared. The Cs/Ru molar ratio and the role of the cesium precursor salt used were studied. Ruthenium and cesium were introduced by the incipient wetness impregnation method using aqueous solutions of ruthenium(III) chloride ($RuCl_3 \cdot nH_2O$) and cesium hydroxide (CsOH) or cesium chloride (CsCl), as accordingly. All the catalysts prepared here possess a constant ruthenium loading of 0.000745 mol $g_{support}^{-1}$ and different Cs/Ru molar ratios (1:1, 0.5:1, and 0.1:1) using cesium hydroxide as precursor salt. Another catalyst with a Cs/Ru molar ratio of 0.1:1 was also prepared with cesium chloride to study the role of the precursor salt. The nominal compositions of the prepared catalysts (wt %) are included in Table 1.

First, the cesium aqueous solution was added to the pelletized support (0.85−1.00 mm) and air-dried. Then the ruthenium aqueous solution was added and after air drying, the catalyst precursors were obtained. Finally, the precursors were sulfided in situ at atmospheric pressure with a H_2S/N_2 (10/90%) flow of 60 mL min^{-1} by heating from room temperature (r.t.) to the sulfidation temperature (Ts) (2 h) at a heating rate of 10 °C min^{-1} to obtain the sulfided catalysts.

The catalyst precursors will be referred to as *x*Cs*y*Ruprec, *x*:*y* being the Cs/Ru molar ratio. The sulfided catalysts will be referred to as *x*Cs*y*RuSTs, where Ts stands for the sulfidation temperature in °C. Moreover the catalyst prepared from cesium chloride will be denoted as 0.1Cs1RuSTs (Cl).

2.3. Characterization of Catalysts. X-ray diffraction patterns (XRD) of the precursor, sulfided, and spent catalysts were obtained with an X'Pert PRO MPD Philips diffractometer (PANanalytical), using monochromatic CuKα radiation (λ = 1.5406 Å). The Kα_1 radiation was selected with a Ge (111)

dx.doi.org/10.1021/cs100053e |*ACS Catal.* 2011, 1, 175–186

primary monochromator. The X-ray tube was set at 45 kV and 40 mA.

Transmission electron micrographs of the precursor and sulfided catalysts were obtained by using a Philips CM 200 Supertwin-DX4 microscope. Samples were dispersed in ethanol and a drop of the suspension was put on a Cu grid (300 mesh).

The textural properties (S_{BET}, V_p, d_p) of the sulfided catalysts were obtained from the N_2 adsorption−desorption isotherms at −196 °C measured with a Micromeritics ASAP 2020 apparatus. Prior to the measurements, samples were outgassed at 200 °C and 10^{-4} mbar overnight. Surface areas were determined by using the Brunauer−Emmet−Teller (BET) equation and a nitrogen molecule cross section of 16.2 Å^2. The pore size distribution was calculated by applying the Barret−Joyner−Halenda (BJH) method to the desorption branch of the N_2 isotherm. The total pore volume was calculated from the adsorption isotherm at $P/P_0 = 0.95$.

X-ray photoelectron spectra of the sulfided and spent catalysts were collected using a Physical Electronics PHI 5700 spectrometer with non monochromatic AlKα radiation (300 W, 15 kV, and 1486.6 eV) with a multichannel detector. Spectra of pelletized samples were recorded in the constant pass energy mode at 29.35 eV, using a 720 μm diameter analysis area. Charge referencing was measured against adventitious carbon (C 1s at 284.8 eV). A PHI ACCESS ESCA-V6.0 F software package was used for acquisition and data analysis. A Shirley-type background was subtracted from the signals. Recorded spectra were always fitted using Gaussian−Lorentzian curves to determine the binding energies of the different element core levels more accurately.

Hydrogen temperature-programmed reduction (H_2-TPRS) of the sulfided catalysts were carried out between 50 and 800 °C using a flow of 10% H_2/Ar (48 mL min^{-1}) and a heating rate of 10 °C min^{-1}. Prior to the analysis, the precursors were sulfided in situ at 500 °C (2 h) using a flow of H_2S/N_2 (10/90% with a flow rate of 60 mL min^{-1}). After that, a helium flow (60 mL min^{-1}) was passed for 30 min at 50 °C to clean the sample.Water produced in the reduction reaction was eliminated by passing the gas flow through a coldfinger (−80 °C). The H_2-TPRS experiments were registered by using an online quadrupole mass spectrometer Balzer GSB 300 02.

Elemental chemical analysis was performed for spent catalysts with a LECO CHNS 932 analyzer to determine the sulfur and the nitrogen content present after the catalytic test through the combustion of the samples at 1100 °C in pure oxygen to form NO and SO_2.

DRIFT spectra of adsorbed NO on spent catalysts were recorded with a Jasco FT/IR-6300 spectrophotometer (equipped with a Harrick diffuse reflectance accessory HVC-DRP cell) at room temperature and NO pressure of 2 bar. Prior to NO adsorption, the spent catalysts were subjected to a soft surface cleaning by H_2 reduction (heating ramp 15 °C min^{-1} up 350 °C and then cooling down to r.t. with He).

The amount of coke deposited on the spent catalysts was determined by measuring the O_2 consumed during temperature-programmed oxidation (TPO), carried out in a Micromeritics TPR/TPD 2900 instrument as well as by measuring the weight change in the catalysts during TPO in a O_2/N_2 (20/80%) gas mixture carried out with a thermogravimetric TGA/SDTA851 equipment (Mettler Toledo). Each sample (ca. 20 mg) was previously heated in He flow at 550 °C for 1 h to homogenize coke and remove the volatile compounds. Once the sample was cooled to ambient temperature in the same flow of He, a burning of coke was carried out by raising the sample temperature to a final temperature of 900 °C at a rate of 10 °C min^{-1}.

2.4. Catalytic Test. The HDS of DBT was chosen for the catalytic test, which was performed in a high-pressure fixed-bed continuous-flow stainless steel catalytic reactor (9.1 mm in diameter, and 230 mm in length), operated in the down-flow mode. The reaction temperature was measured with an interior placed thermocouple in direct contact with the catalyst bed. The organic feed was adjusted to solutions in *cis*-, *trans*-decalin of DBT (10000 ppm). Each solution was supplied by means of a Gilson 307SC piston pump (model 10SC). For the activity tests, 0.5 g of catalyst were used (particle size 0.85−1.00 mm) and were diluted with silicon carbide (0.85 mm) to 3 cm^3. Prior to the activity test, the catalyst precursors were sulfided at atmospheric pressure with a H_2S/N_2 (10/90%) flow of 60 mL min^{-1} by heating from r.t. to the sulfidation temperature (Ts) (2 h) at a heating rate of 10 °C min^{-1}. Catalytic activities were measured at different temperatures (300−440 °C), under 3.0 MPa of H_2, with a flow rate of 100 mL min^{-1} and with hourly space velocities (WHSV) of 32 h^{-1}. The evolution of the reaction was monitored by collecting liquid samples after 60 min at the desired reaction temperature. These liquid samples were kept in sealed vials and subsequently analyzed by gas chromatography (Shimadzu GC-14B, equipped with a flame ionization detector and a capillary column, TBR-14, coupled to an automatic Shimadzu AOC-20i injector).

For these catalysts, the main products of the HDS reaction were biphenyl (BP), cyclohexylbenzene (CHB), bicyclohexyl (BCH), benzene (B), and cyclohexane (CH). The total conversion of HDS reaction was calculated from the ratio of converted DBT/initial DBT. The selectivity to the different reaction products was calculated considering BP, CHB, B, and CH as the only products obtained for HDS. Assuming that the reaction is pseudo-first order, then the reaction rate constants of HDS (k_{HDS}) were calculated according to the eq 1:

$$k_{HDS} = -(F/W)\ln(1-x) \quad (1)$$

in which, F is the feed rate of dibenzothiophene (mol min^{-1}), W is the catalyst weight (g), and x is the fractional conversion.

Activity at steady-state conditions is described in terms of quasi-turnover frequency (QTOF) using a specific reaction rate according to eq 2:

$$r = [X \cdot F]/m \quad (2)$$

where r is the specific rate (mol mol$_{Me}^{-1}$ s^{-1}), X is the conversion of DBT, F is the molar flow rate of this reactant (mol s^{-1}), and m refers to the metal atoms per gram of catalyst (mol$_{Me}$ g$_{cat}^{-1}$)

3. RESULTS AND DISCUSSION

3.1. Characterization of Catalysts. *3.1.1. XRD.* Figures 1A and 1B depict the XRD profiles of the catalysts sulfided at 500 and 600 °C, respectively. From such diffractograms it can be observed, in all cases, reflection lines at 2θ (deg) values of 31.8, 45.7, and 54.2 corresponding to the [200], [220], and [311] crystallographic planes, respectively, of the RuS_2 phase in a pyrite type structure (PDF 00-0120737), which is present in all the samples. Both, the catalysts sulfided at 500 and 600 °C, also present reflection lines at 30.7 and 54.6° due to the [110] and [211] crystallographic planes of the CsCl compound [PDF 00-001-0935],

dx.doi.org/10.1021/cs100053e |*ACS Catal.* 2011, 1, 175–186

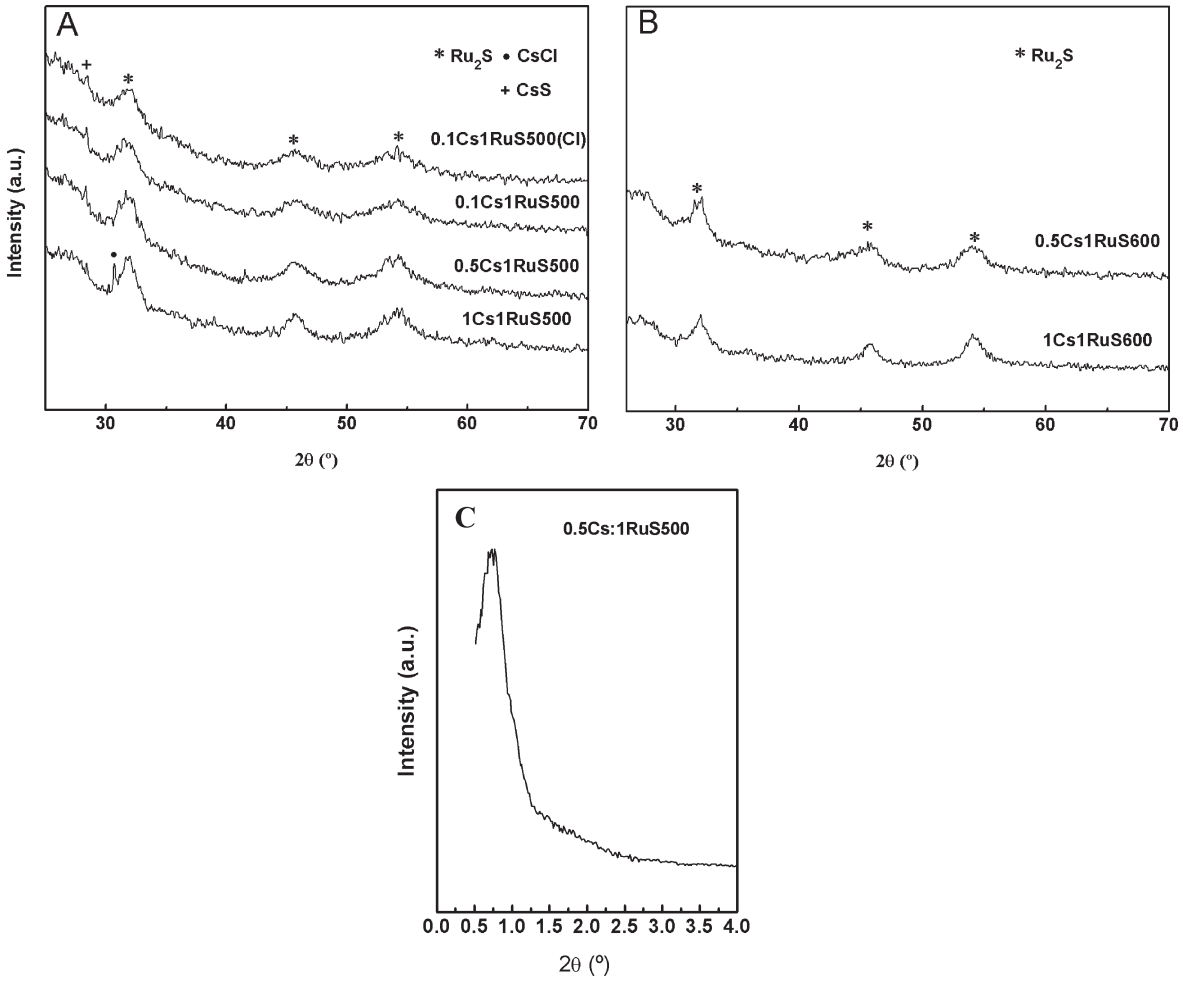

Figure 1. X-ray diffractograms of catalysts sulfided at (A) 500 °C; (B) 600 °C; and (C) 0.5Cs:1RuS500 at low angles.

this signal being more intense for the catalysts with higher cesium content. This suggests that CsOH reacts with $RuCl_3$ to form CsCl. Moreover, the catalysts sulfided at 500 °C present another weak reflection line, which can be ascribed to the CsS phase and whose 2θ value is 28.2° corresponding to its [121] crystallographic plane [PDF 00-033-0377]. If we compare the XRD reflection lines of the RuS_2 phase at both sulfidation temperatures, at 600 °C, they are more intense indicating that the RuS_2 particles become more crystalline and, possibly, with a bigger particle size in comparison to the catalysts sulfided at 500 °C.[26]

If we study the influence of the cesium content (Figure 1A), it is seen how the higher the cesium content the better defined are the RuS_2 diffraction lines and therefore, the lower the dispersion. Moreover, the diffractogram of the catalyst prepared from CsCl, 0.1Cs1RuS500 (Cl), is similar to that prepared from CsOH.

XRD profiles of spent catalysts were also recorded (not shown). The RuS_2 reflections lines were maintained after the catalytic test, indicating the stability of the RuS_2 particles formed after the sulfidation process. Only these signals are slightly less intense for the spent catalysts sulfided at 500 °C, indicating a slight loss of crystallinity of the active phase during the catalytic test. It has been reported that amorphous RuS_2 can be reduced under the reaction conditions[27] although such reduction was not observed from XRD patterns. However, if metallic Ru particles are formed, they are too small to be detected by XRD.

3.1.2. TEM. Transmission electron microscopy (TEM) was performed to elucidate the distribution of the active phase on the support. In general, it can be said that TEM analysis shows a heterogeneous distribution of the active phase, whose dispersion is totally dependent on cesium loading.

The micrographs belonging to 1Cs1RuSTs catalyst are shown in Figures 2A and 2B. At first glance, the micrographs show zones where there are big agglomerates on the external surface, assigned to the RuS_2 active phase according to EDAX analysis. Although there are some particles inside the pores, the dispersion of the active phase in the whole support is poor, in a greater extend in the catalyst sulfided at 500 °C. The catalyst sulfided at 600 °C also presents zones where agglomerates are present. However, a greater proportion of highly dispersed particles are clearly observed. Moreover, the analysis by EDAX in some zones of dispersed particles gave Cs/Cl atomic ratios close to 1 arising from the presence of CsCl compound, as detected by XRD.

The sample with a Cs/Ru molar ratio of 0.5:1, presents micrographs (Figures 2C and 2D) where the dispersion of the RuS_2 phase is better, although agglomerates are still present but to a lesser extend than before. The catalyst sulfided at 500 °C possesses an alignment of the particles as can be clearly seen in Figure 2C indicating that they are mainly located inside the pores of the support. The sample sulfided at 600 °C (Figure 2D) presents a lower homogeneity than that observed with the sample

dx.doi.org/10.1021/cs100053e |*ACS Catal.* 2011, 1, 175–186

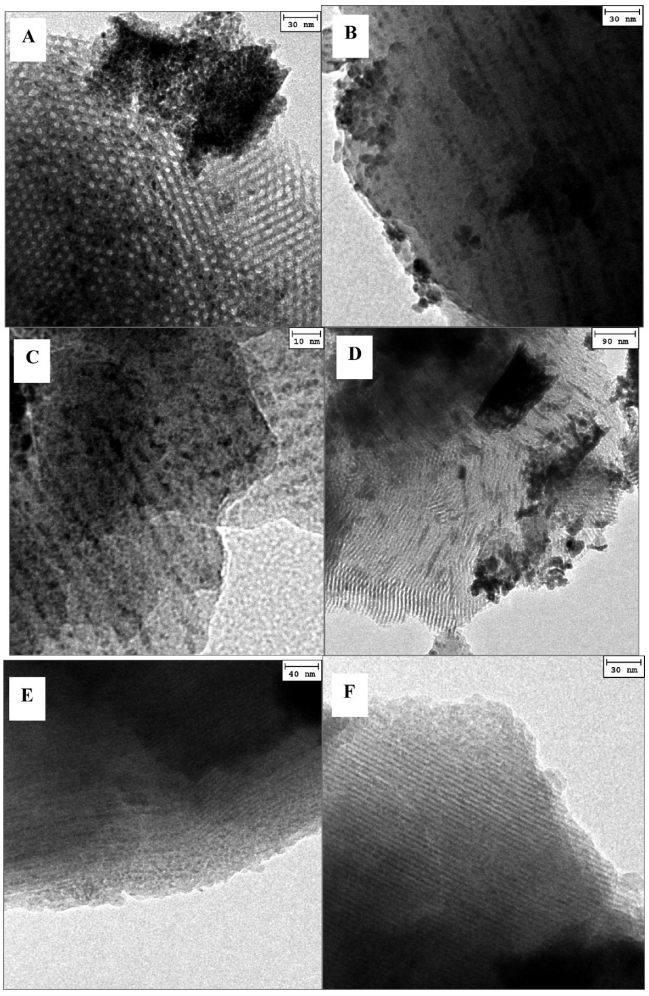

Figure 2. TEM micrographs for (A) 1Cs1RuS500, (B) 1Cs1RuS600, (C) 0.5Cs1RuS500,(D) 0.5Cs1RuS600, (E) 0.1Cs1RuS500, and (F) 0.1Cs1RuS500 (Cl).

sulfided at 500 °C. In this sense, the 0.5Cs1RuS600 sample possesses a greater proportion of RuS_2 agglomerates, which means a scant dispersion of such a phase as well. However, when diminishing the cesium loading until a Cs/Ru ratio of 0.1:1, the dispersion of the active phase increases conspicuously, as can be clearly seen from Figure 2E, where particles smaller than 10 nm are highly dispersed and located inside the channels. Besides, the catalyst prepared from CsCl precursor salt, 0.1Cs:1RuS500 (Cl), also presents a high dispersion of the active phase, Figure 2F, similar to that prepared from CsOH.

The data presented here reveal that the lower the cesium content, the better the dispersion of the active phase. Moreover, the cesium precursor salt does not affect the active phase in terms of dispersion.

3.1.3. Textural Properties. Textural properties of the support and sulfided catalysts such as BET surface area, pore volume, and mean pore diameter were measured by N_2 adsorption−desorption isotherms at −196 °C, and the corresponding data are summarized in Table 1. In all cases the isotherms maintain the same features as that of the support, that is, they all are of type IV in accordance to IUPAC classification, typical of mesoporous materials, which indicates that after metal incorporation the mesoporous structure of the support is maintained.

From data compiled in Table 1, it can be noticed that the textural properties diminish after the impregnation and sulfidation processes. Such a decrease is mainly due to the blocking of the porous structure after the incorporation of the precursor salts and subsequent formation of the corresponding sulfides. TEM micrographs of sulfided catalysts have revealed that the higher the cesium loading, the higher the RuS_2 agglomerates, which provokes a blockage on the pores surface that hinders the access of nitrogen molecules. Moreover, the mean pore diameter also suffers a decrease but to a lesser extent. This is explained considering that agglomerates are blocking the entrance of some pores; however, there are other ones where the metals are not deposited and are able to adsorb N_2 at −196 °C, as can be clearly seen by TEM micrographs. In general, 1Cs1RuSTs and 0.5Cs1RuSTs sulfided catalysts display zones with big size agglomerates, other zones where highly dispersed particles are presented, and other ones where the pristine support is clearly noticeable. The catalysts with a 0.1Cs/1Ru molar ratio present the highest BET surface area and pore volume values. This is explained by the high dispersion found from TEM analysis where the distribution of the active phase is found to be highly homogeneous, little particles perfectly aligned and mainly located inside the pore structure that do not provoke a drastic blockage of the surface area but slightly diminish the mean pore diameter.

3.1.4. XPS. X-ray photoelectron spectroscopy (XPS) analyses were performed to evaluate the chemical state of the superficial elements. To this end O 1s, Si 2p, Ru 3p, S 2p, Cs 3d, and Cl 2p signals were analyzed for precursors, sulfided, and spent catalysts, and the corresponding binding energy values are lumped together in Table 2. Regarding the BE values of O 1s (532.8 eV) and Si 2p (103.4 eV), they were maintained practically constant for all the samples, revealing the high stability of the support during the whole process. The Cs $3d_{5/2}$ BE values of the catalyst precursors, 0.1Cs1Ruprec and 0.1Cs1Ruprec (Cl), were of 724.2 and 723.9 eV, respectively, and assigned to the presence of CsOH and CsCl, respectively.[28] After sulfiding, the Cs $3d_{5/2}$ maxima reaches values ranged between 724.0 and 725.9 eV, ascribed to the presence of cesium sulfides with different stoichiometry, Cs_2S_{2n} (n = 1, 2, 3).[29,30] From XRD patterns the cesium sulfide detected was CsS.

Ruthenium species were analyzed by recording the Ru $3p_{3/2}$ spectrum of the samples and studied by an appropriate curve fitting. Figure 3A depicts the XPS spectra of the precursor and 0.1Cs1RuS500 sulfided catalyst, as representatives. The Ru $3p_{3/2}$ signal of the catalyst precursor is slightly asymmetric and can be fitted by two contributions. The first centered at 463.0 eV attributed to $RuCl_3 \cdot 3H_2O$ and the other one, of low intensity, localized at about 465.5 eV ascribed to RuO_xCl_y type compounds that contain Ru(IV) owing to, probably, the oxidation of the precursor salt during the preparation of the sample,[31] as observed before.[32] After the sulfiding process, the Ru $3p_{3/2}$ signal shifted to lower BE values and as a result of its spectral fitting, two contributions were identified, one centered between 460.9 and 462.0 eV and a second one at 463.4−463.9 eV. The former and main contribution is assigned to the RuS_2 compound; meanwhile the weakest contribution was attributed to Ru^{n+} compounds. On the other hand, XRD and EDAX analysis have pointed to the formation of CsCl compound. The absence of the Cl 2p signal suggests that this compound is mainly located inside the support chanels.

The influence of sulfiding temperature is observed in Figure 3B for 1Cs1RuSTs catalysts. The intensity of the Ru $3p_{3/2}$ contribution attributed to RuS_2 compound increases when the sulfiding

dx.doi.org/10.1021/cs100053e |*ACS Catal.* 2011, 1, 175–186

Table 2. XPS Spectral Parameters

	binding energy (eV)								
	Ru $3p_{3/2}$				S $p_{3/2}$				
samples	$RuCl_3$	RuO_xCl_y	RuS_2	Ru^{n+}	RuS_2	Cs_2S_{2n}	Cs $3d_{5/2}$	Cl $2p_{3/2}$	S/Ru atomic ratios
Catalyst Precursors									
0.1Cs1Ruprec	462.9	465.5					724.2	198.7	
0.1Cs1Ruprec (Cl)	463.0	465.5					723.9	198.4	
Sulfided Catalysts									
1Cs1RuS500			461.6	463.6	162.5	164.5	724.3		2.7
1Cs1RuS600			462.0	463.9	162.5	163.8	725.1		3.1
0.5Cs1RuS500			461.3	463.8	162.4	164.6	724.0		2.7
0.5Cs1RuS600			461.5	463.5	162.3	163.5	724.9		2.4
0.1Cs1RuS500			461.0	463.4	162.0		724.6		2.6
0.1Cs1RuS500 (Cl)			460.9	463.5	161.7		724.5		1.5
Spent Catalysts									
1Cs1RuS500			461.7	463.7	162.5	163.9	724.2		2.0
1Cs1RuS600			462.0	463.6	162.2	163.3	725.6		2.1
0.5Cs1RuS500			461.2	463.5	162.0	162.7	724.5		1.8
0.5Cs1RuS600			461.3	463.6	162.1	162.7	724.5		1.8
0.1Cs1RuS500			461.2	463.4	161.8		724.7		1.9
0.1Cs1RuS500 (Cl)			461.0	463.5	161.8		724.7		1.4

temperature does; meanwhile the intensity of the Ru^{n+} contribution decreases. Such behavior is explained by the formation of more RuS_2 phase at higher temperature poorly dispersed as observed from TEM micrographs. The influence of cesium content on the Ru 3p signal is observed in Figure 3C. It is clearly noticeable how the Ru 3p signal intensity decreases when Cs loading does. These results are in accordance with those previously observed from TEM, that is, high cesium loadings provoke an agglomeration of the RuS_2 particles on the external surface. Therefore, when the content of cesium decreases, the RuS_2 phase locates preferentially inside the pores without being detected by the XPS technique, and hence the intensity of the Ru 3p signal decreases.

The S 2p signal was also evaluated (Figure 4) where the S $2p_{3/2}$ and S $2p_{1/2}$ doublet is present. The fit gave as result two main contributions to the S $2p_{3/2}$ signal: the first one with BE values between 161.7 and 162.5 eV, and a second one placed between 163.3 and 164.6 eV. The former is assigned to sulfur forming S_2^{2-} anions according to previous works[33] and coming from RuS_2 compound in a pyrite like structure, which is present in all catalysts. The signal at higher BE values (163.3 to 164.6 eV) is ascribed to cesium sulfide, where the S−S bond interaction is important, that is, Cs_2S_{2n} type molecules.[30]

The influence of the sulfiding temperature on the S 2p signal is observed in Figure 4A. As observed before with the Ru 3p signal, an increase in the sulfiding temperature causes an increase in the contribution ascribed to the RuS_2 compound; while the contribution assigned to Cs_2S_{2n} compounds shifts to lower binding energy values pointing to the formation of cesium sulfide with a different stoichiometry. The influence of cesium loading is observed in Figure 4B where the same trend than that seen in the Ru 3p spectra is observed, that is, the intensity of the S 2p signal decreases while diminishing the cesium content because of the formation of highly dispersed particles.

The analysis of spent catalysts revealed that the BE values hardly changed, while the Ru 3p and S 2p signals diminished on intensity. Such a feature could be due to the covering by residual coke while the decrease of the S 2p signal could also be ascribed to the loss of sulfur during the catalytic test, as reported by others,[27] as long as under reducing conditions, RuS_2 can be transformed into metallic ruthenium. From data reported here, no evidence of metallic ruthenium formation was found, so only a partial sulfur loss could be happening here.

Table 2 also includes the superficial S/Ru atomic ratios. Except for the catalyst prepared from CsCl, all of them exhibit values higher than the theoretical one of 2.0. Berhault et al.[34] pointed out that the sulfur excess on RuS_2/SiO_2 catalysts is due to different Ru superficial species remaining after the sulfiding procedure having 1, 2, 3 or more sulfur vacancies presented on the surface, and could be responsible for the Ru $3p_{3/2}$ contribution located at higher binding energies assigned to Ru^{n+} species. The S/Ru atomic ratios decrease after the catalytic run, until values are close to 2.0 in all cases, indicating both a slight loss of sulfur during the test that could come from Ru^{n+} species and the stability of the RuS_2 phase, as also observed from XRD data. Finally, the XPS survey spectra of Cs-promoted Ru catalysts show that the Cs 4d and Cs 4p lines overlap with the S 2p photoelectron lines. In such a case, the comparison of the atomic ratios between Cs-promoted and Cs-free catalysts is not reliable.

3.1.5. H_2-TPRS. H_2-TPRS is an important tool for determining the sulfur species present and the sulfurization degree, as well as the stability of the active phase on the catalyst.[35,36] The TPRS curves are depicted in Figure 5, where the H_2S elimination as a function of the time and temperature under a reducing atmosphere (Ar/H_2) is shown. In general, all of them follow the same trend, while the position and intensity of the peaks depend on cesium quantity. The fit of all TRPR-H_2 curves gave as a result three bands (A, B, and C). Peak A has been ascribed to the

dx.doi.org/10.1021/cs100053e |*ACS Catal.* 2011, 1, 175–186

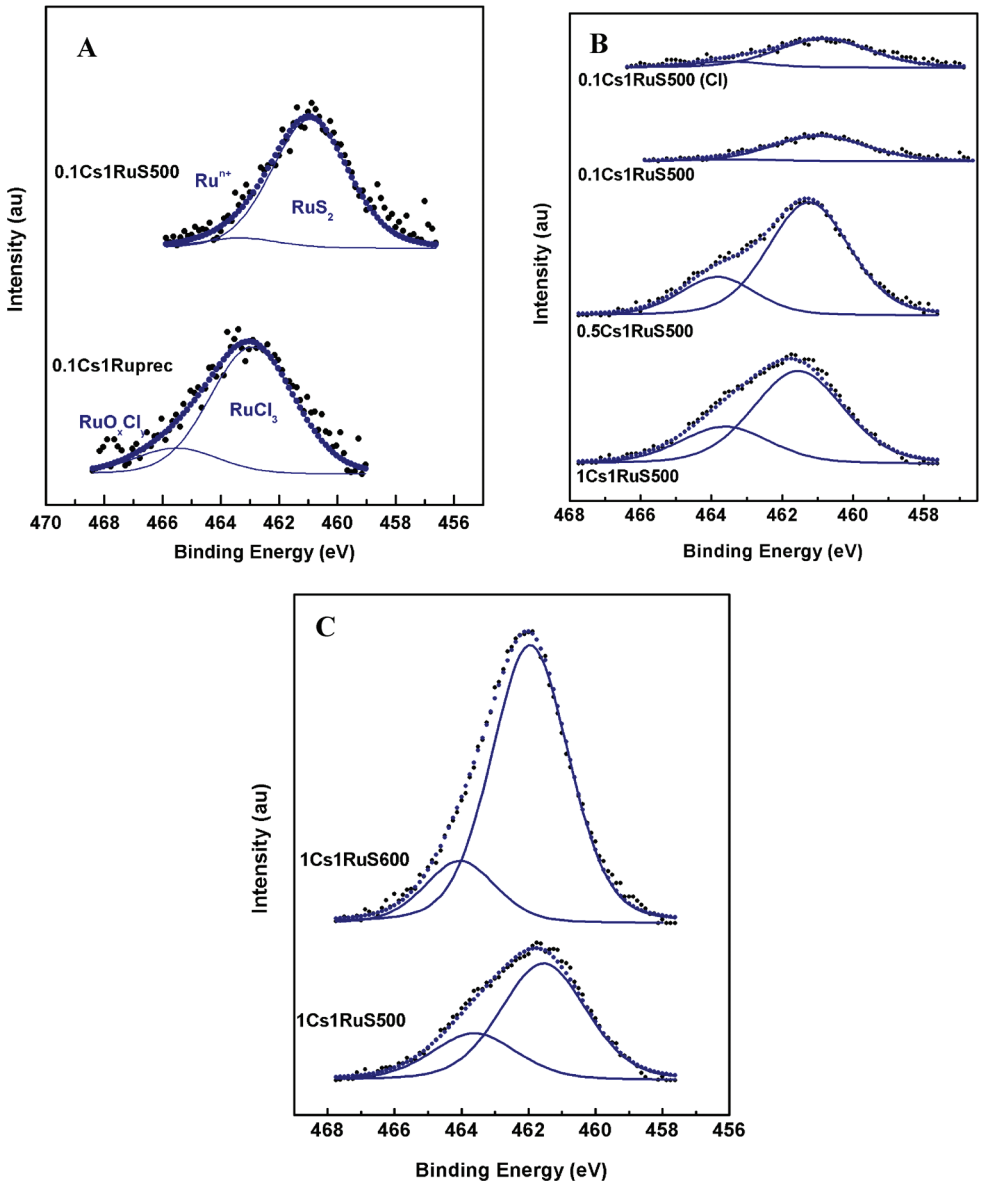

Figure 3. Ru $3p_{3/2}$ core level spectra for (A) 0.1Cs1Ruprec and 0.1Cs1RuS500 sulfided catalyst; (B) catalysts sulfided at 500 °C with different Cs/Ru molar ratios; and (C) 1Cs1RuSTs catalysts.

recombination of SH^- species,[19] although some authors have observed that this band tends to disappear when the sulfiding temperatures are higher, suggesting that such a band originated from reduction of an amorphous or poorly crystalline phase synthesized at low temperatures.[26] Peaks B and C are ascribed to the reduction of bulk RuS_2 phase leading to ruthenium metallic phase.[19,35]

In accordance with the H_2-TPRS curves, the higher the cesium content, the lesser are the band intensities; moreover, the maxima of the curves are shifted to higher temperatures. In this regard, the 0.1Cs1RuS500 sample profile exhibits the most intense H_2S-release pattern that occurs at lower temperatures than that for the 1Cs1RuS500 catalyst. Taking into account the features observed in Figure 5, it implies that the cesium content is the main reason of a low H_2S elimination, that is, a minor amount of labile sulfur is present on the catalysts. Moreover, if we compare the catalysts with Cs/Ru molar ratio of 0.1:1 but prepared from different cesium precursor salts, it is clearly seen that the TPRS pattern of 0.1Cs1RuS500 (Cl) is much less intense although with the same feature than that observed in the case of the 0.1Cs1RuS500 catalyst. Therefore, the cesium precursor salt employed also plays a key role in the sulfur lability.

3.2. Catalytic Results. All the catalysts were tested in the HDS reaction of DBT, and their catalytic performance was monitored in a temperature range of 260−440 °C. The DBT HDS reaction generally occurs in two different pathways:[37] the first one, called direct desulfurization (DDS) route, gives rise to biphenyl as the main product and the second one is the hydrogenation route that leads to cyclohexylbenzene (CHB) as the main product.

The HDS rate constants calculated according to eq 1 are plotted in Figure 6a and 6b. Figure 6a depicts the k_{HDS} against the reaction temperature for the 1Cs1RuSTs and 0.5Cs1RuSTs catalysts, sulfided at 500 and 600 °C. In general, when the reaction temperature increases, so does the k_{HDS}. Such a phenomenon may be explained by the formation of CUS sites during the

dx.doi.org/10.1021/cs100053e |*ACS Catal.* 2011, 1, 175–186

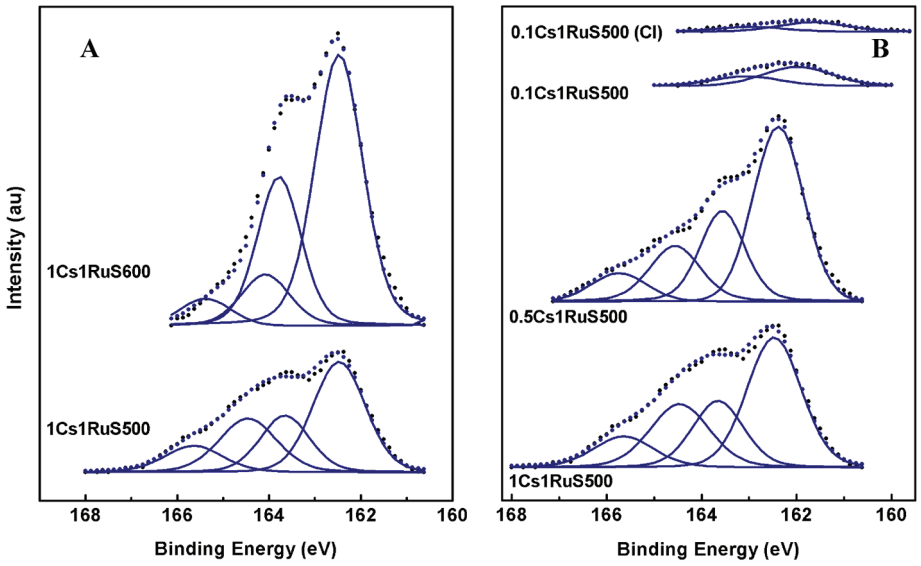

Figure 4. S 2p core level spectra for (A) 1Cs1RuSTs catalysts and (B) Catalysts sulfided at 500 °C with different Cs/Ru molar ratios.

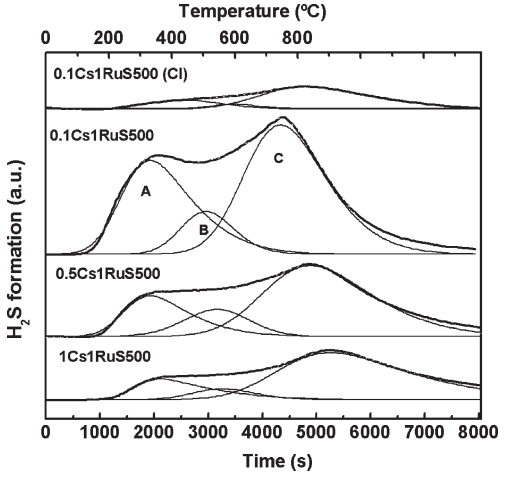

Figure 5. H_2-TPRS patterns of the catalysts sulfided at 500 °C.

catalytic reaction; furthermore, the reducing conditions employed in the catalytic test, in accordance with previous works,[38] are responsible for such active sites creation, of great importance in the HDS reaction of transition metal sulfides.[39]

Sulfiding temperature is of paramount importance in the formation of the active phase and therefore in the catalytic activity of the samples, and Figure 6a depicts such influence. The catalysts prepared with a 1:1 Cs/Ru molar ratio (1Cs1RuSTs) show similar catalytic activities at both sulfiding temperatures, that is, at 500 and 600 °C, although at 500 °C a slight lower catalytic activity is observed. It seems that the sulfiding process at higher temperature does not have enough influence on the catalytic activity because of the formation of big RuS_2 clusters, poorly dispersed on the external surface of the support at both sulfiding temperatures, as can be observed on TEM micrographs (Figure 2). However, as the molar ratio diminishes (0.5Cs1Ru) a sulfiding temperature of 600 °C provokes a decrease in the k_{HDS}, mainly at high reaction temperatures, mainly because of a higher agglomeration of the active phase at this sulfiding temperature (600 °C). It must also be mentioned that a catalyst with a 2:1 (Cs/Ru) molar ratio was synthesized to observe its catalytic performance as the cesium quantity increased 2-fold the amount of ruthenium, since some authors have suggested that this ratio is optimal for ruthenium sulfided systems.[22] As expected, according to the preceding results the observed catalytic activity was very low.

With these premises it was considered important to prepare other catalysts with a lower cesium content 0.1:1 (Cs/Ru) using cesium hydroxide (0.1Cs1RuSTs) and cesium chloride (0.1Cs1RuSTs (Cl) as cesium precursor salts. Although it was not observed an important amelioration in the catalytic activity by increasing the sulfiding temperature 100 °C, the catalytic activity of both these catalysts was also studied at a sulfiding temperature of 600 °C. The catalytic results are depicted in Figure 6b. The samples sulfided at 500 °C follow the same trend at all reaction temperatures; the k_{HDS} values attained are in all cases very close, although at 360 °C the catalysts prepared from cesium hydroxide exhibit a much higher HDS activity. The textural and structural properties of both catalysts are similar according to XRD, S_{BET}, and TEM analysis, that is, they both present the same dispersion of the RuS_2 active phase. Notwithstanding, the results extracted from TPRS results (Figure 5) point to the different sulfur lability on both catalysts, in spite of the similar catalytic activity of both catalysts at temperatures lower than 360 °C.

The influence of the cesium precursor salt is more evident when the catalysts are sulfided at 600 °C (Figure 6b) where the difference found are very important, the catalysts prepared from cesium hydroxide being much more active. Moreover if we compare the catalytic results with a Cs-free RuS_2/Si-SBA catalyst prepared and tested in the same conditions,[24] the negative effect of the Cs addition to a mesoporous material is again reflected. The cesium-free catalyst presented a k_{HDS} at 360 °C of 10.84×10^5 mol g^{-1} min^{-1} while the most active catalyst prepared here possesses a value of 7.85×10^5 mol g^{-1} min^{-1}.

The catalytic results along with the characterization data suggest that the activity of ruthenium sulfide catalysts doped with cesium using mesoporous supports mainly depends on the dispersion of the active phase attained.

Taking into account the catalyst deactivation during time on-stream (TOS) operation, we calculated the quasi-turnover

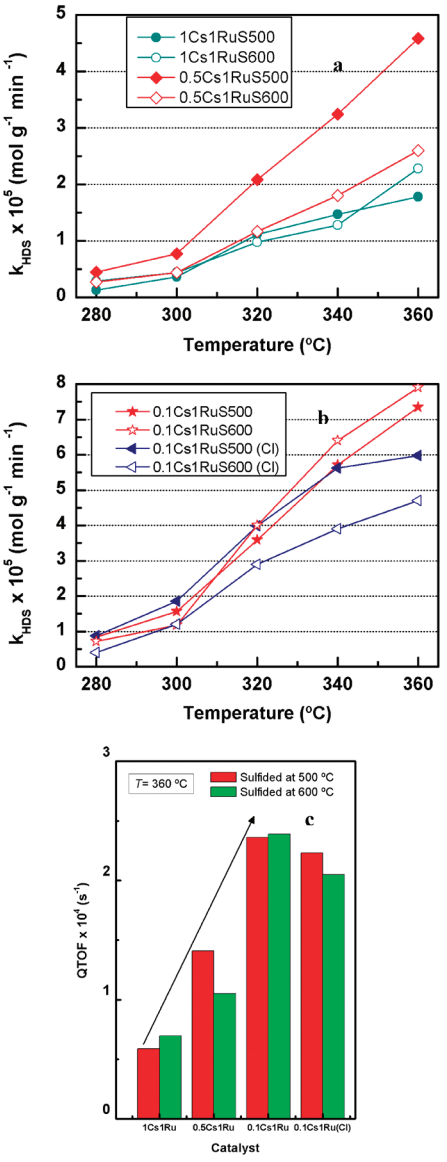

Figure 6. Evolution of the k_{HDS} versus reaction temperature for (a)1Cs1RuSTs and 0.5Cs1RuSTs catalysts, sulfided at 500 and 600 °C; and (b) 0.1Cs1RuS500 and 0.1Cs1RuS500 (Cl); (c) QTOF for the catalysts at a reaction temperature of 360 °C.

frequency (QTOF) values from the specific reaction rates at steady-state expressed as moles of molecules converted per second and per moles of metal (eq 2). The QTOF values of the catalysts are compared in Figure 6c. As seen in this figure, and according to the preceding results, the QTOF of the catalysts sulfided at 500 °C follows the trend 0.1CsRu > 0.5Cs1Ru > 1Cs1Ru, indicating that the intrinsic activity decreased with an increase of the Cs loading.

The selectivity results obtained here show that all catalysts follow the DBT HDS reaction through the DDS route, biphenyl even being the unique reaction product found for the catalysts with higher cesium loadings, in line with the results reported by Ishihara.[40] Only the catalysts with a 0.1Cs:1Ru molar ratio presented a BP selectivity of 90% while the selectivity to the hydrogenation route product, cyclohexylbenzene, was of only 10%. The enhancement of hydrogenation in the HDS of the DBT reaction over these catalysts is because of the formation of

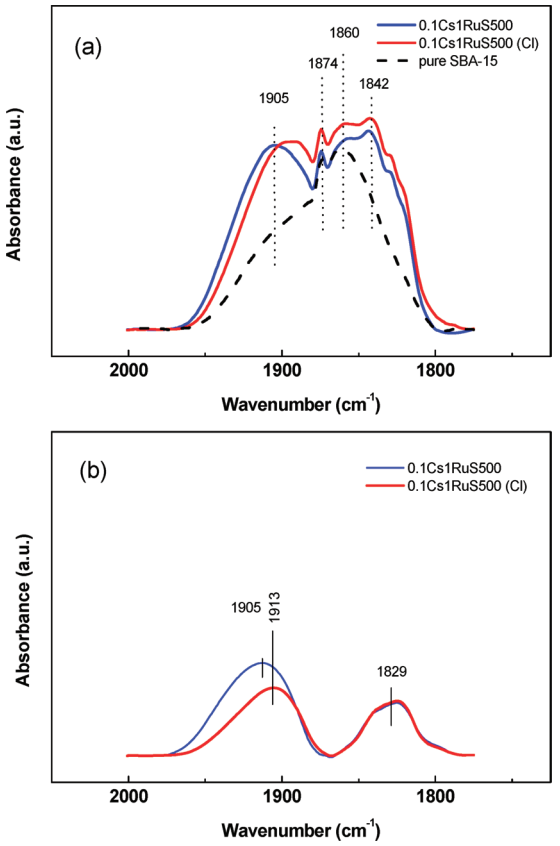

Figure 7. Influence of Cs precursor salt on the DRIFT spectra of NO adsorbed at room temperature for 10 min onto 0.5Cs1RuS500 (from CsOH) and 0.5Cs1RuS500(Cl) (from CsCl) catalysts: (a) the spectra of spent catalysts (after HDS at 360 °C) and pure SBA-15 support, (b) the difference spectra obtained after subtraction of NO adsorbed on pure support.

smaller RuS_2 crystallites on the surface of these catalysts with respect to other samples, as evidenced by XRD (vide supra). This is because the small RuS_2 particles show some preferential exposed planes, favoring hydrogenation properties, as already mentioned for alumina-supported ruthenium sulfide catalysts.[14,19]

3.3. Catalyst Activity-Structure Correlation. The characterization and catalytic results indicate that the addition of cesium to a mesoporous material does not have a beneficial effect in the sense that the higher the cesium content the lower the dispersion of the active phase and therefore the lower the catalytic activity in the DBT HDS reaction. Our results are contrary to those previously published in the literature. Ishihara et al., in a first work,[41] studied the addition of alkali metal hydroxides to alumina-supported ruthenium catalysts. They found that by increasing the amount of alkali metal hydroxides in the alumina-supported ruthenium system, the conversion of DBT increased and reached the maximum at M/Ru = 2 (M = Na or Cs). Further additions decreased the activity. Among the studied alkali metals (Li, Na, K, Rb, and Cs), the cesium promoted catalyst was the most active. They reported that the location of cesium is close to the ruthenium species, and the dispersion of ruthenium species increases with an increase in the Cs/Ru ratio; furthermore, the presence of cesium in close proximity to ruthenium atoms strengthens the bond of ruthenium and sulfur, stabilizing ruthenium sulfide. In later works,[21,42] they elucidated the behavior of sulfur on the ruthenium catalysts and the role of cesium in HDS by

dx.doi.org/10.1021/cs100053e |ACS Catal. 2011, 1, 175–186

radioisotope tracer methods, concluding that the mobility of sulfur on the catalysts decreased by the addition of cesium. On the contrary, the amount of labile sulfur on the catalyst increased with the amount of cesium added and reached the maximum at Ru/Cs = 1:2 suggesting that the Ru species in the catalyst was successfully dispersed on alumina. Further, it was reported that cesium promoted the C−S bond scission of DBT.

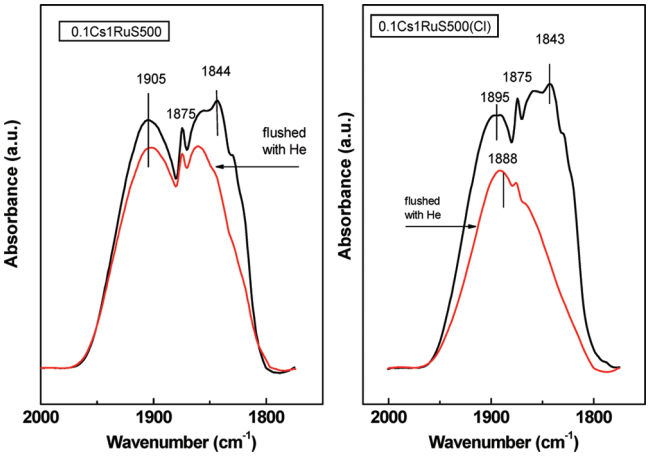

Figure 8. DRIFT spectra of NO adsorbed at room temperature onto 0.1Cs1RuS500 and 0.1Cs1RuS500(Cl) catalysts subjected to flushing with He for 8 min.

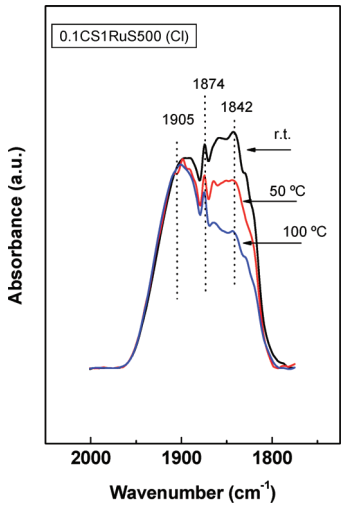

Figure 9. Temperature dependence of DRIFT spectra on spent 0.1Cs1RuS500(Cl) catalyst for NO adsorption in the temperature range of 25−100 °C.

With these premises and considering the characterization and activity results exposed here, it can be pointed out that the role of Cs to RuS_2 hydrotreating catalysts strongly depends on the support used. While the promoter effect of cesium on γ-Al_2O_3 is positive, on a mesoporous material such as SBA-15, the effect is negative. In this sense, the presence of cesium does not favor a good dispersion of the RuS_2 active phase, that is, less cesium atoms are close to ruthenium atoms to stabilize the Ru−S bond and therefore the amount of labile sulfur also decreases by decreasing the dispersion.[42] This is in agreement with our H_2-TPRS experiments that show an increase of the amount of H_2S released with a decrease of cesium content in the catalysts, indicating that sulfur lability is inhibited in the presence of a large amount of Cs on the catalyst surface. The low dispersion of the active phase and the decrease in the sulfur lability might explain the observed decrease in the catalytic activity with an increase of Cs content in the catalysts (vide infra).

Concerning the effect of Cs precursor salts, it was found that the catalyst prepared from cesium hydroxide (0.1Cs1RuSTs) showed the largest activity in HDS at 360 °C with respect to the catalyst prepared from cesium chloride (0.1Cs1RuSTs(Cl)) suggesting that a larger activity of the former sample could be due to its larger amount of CUS sites (Figure 6). Indeed, the H_2-TPRS results of the catalysts sulfided at 500 °C indicate that the sample prepared from CsOH precursor showed larger sulfur lability than its counterpart prepared from cesium chloride (Figure 5). This was confirmed by DRIFT spectroscopy of adsorbed NO for both spent catalysts (Figures 7a and 7b). To the best of our knowledge, up to date, DRIFT spectra of adsorbed NO onto sulfided RuS_2-Cs catalysts are not reported in the literature. Thus, in Figure 7a the DRIFT spectra of NO adsorbed at room temperature onto both spent catalysts (after HDS at 360 °C) are compared with that of NO adsorbed on pure SBA-15 support. As seen in this figure, both catalysts show two bands at 1905 and 1842 cm^{-1} whereas the pure support show one band centered at about 1860 cm^{-1}. Additionally, all spectra show one band centered at 1875 cm^{-1} because of NO adsorbed in its monomeric form in the gas phase.[43] After subtraction of NO adsorbed on the pure support, the spectra of both spent catalysts show two bands at about 1900 and 1840 cm^{-1} (Figure 7b) which could be tentatively ascribed to $(NO)_2$ dimer species adsorbed on the Ru(Cs) sulfide phases. Interestingly, the spectrum of the most active

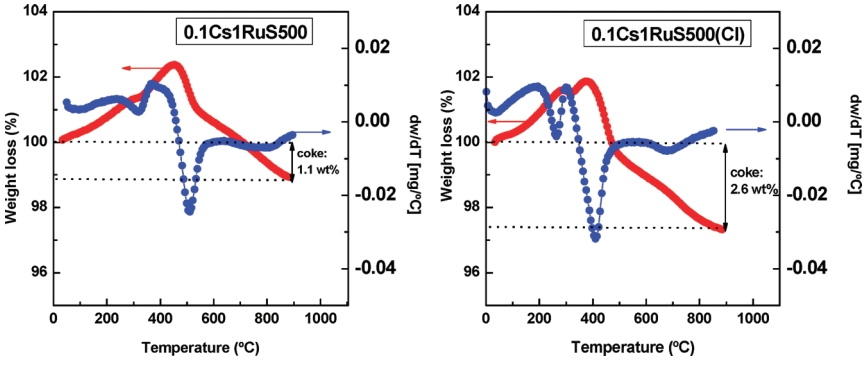

Figure 10. TG/DTG profiles of spent catalysts (0.1Cs1RuS500 and 0.1Cs1RuS500 (Cl)) after DBT HDS reaction. Drop lines mark the limit of weight loss for the calculation of the amount of coke formed.

dx.doi.org/10.1021/cs100053e |ACS Catal. 2011, 1, 175–186

catalyst in the HDS reaction at 360 °C (0.1Cs1RuS500) shows a band at about 1900 cm^{-1} with a larger intensity than that of its counterpart prepared from cesium chloride suggesting the presence of a larger amount of CUS sites.

To compare the strength of the NO adsorption on both catalysts, the surfaces of both catalysts having adsorbed NO were flushed with He for 8 min (Figure 8). As expected, for both catalysts the intensity of the bands decreased, indicating a partial NO desorption from the catalyst surface. It can be seen that the 0.1Cs1RuS500 sample shows two bands due to $(NO)_2$ dimer species. On the contrary, for 0.1Cs1RuS500(Cl) the NO exists in its monomer form (broad band centered at 1890 cm^{-1}) indicating that there is enough strong NO-metal sulfide interaction to prevent NO dimerization. The strong strength of this interaction was confirmed by NO adsorption at increasing temperature (Figure 9). After NO adsorption at 100 °C, the intensity of the band at about 1842 cm^{-1} decreased whereas the intensity of the band at 1905 cm^{-1} remained unchanged.

Finally, it is well-known that the HDS activity can decrease by adsorption of coke precursors on the active sites. In this study, the amount of coke deposited on the spent catalysts was determined by measuring the O_2 consumed during temperature-programmed oxidation (TPO) (figure not shown here) as well as by TPO experiments followed by TGA measurements (Figure 10). As seen in Figure 10, the catalyst prepared from cesium chloride precursor showed a little larger oxygen consumption corresponding to oxidation of coke than its counterpart prepared from cesium hydroxide. From the TPO/TGA measurements, the amounts of coke formed were 1.1 wt % (0.1Cs1RuS500) and 2.6 wt % (0.1Cs1RuS500(Cl)) indicating a larger coke formation on the sample prepared from cesium chloride precursor. This is expected because the presence of residual Cl^- ions on the catalyst surface leads to an increase of the catalyst acidity which favors deactivation by coke formation.

Summarizing, a largest activity of the sample prepared from cesium hydroxide could be explained as due to its largest amount of CUS sites and optimized strength of feed molecules adsorption on CUS sites along with the lower amount of coke present on the catalyst surface.

4. CONCLUSIONS

A family of catalysts based on RuS_2 with different cesium loadings and supported on a mesoporous material (SBA-15) were tested in the HDS of DBT, and the results obtained indicate that (i) the addition of cesium provokes a blockage of the silica mesoporous structure decreasing the dispersion of the RuS_2 active phase, mainly located on the external surface, and therefore decreases the catalytic activity; (ii) the presence of cesium alters the reaction mechanism in a way that only the product coming from the DDS route is obtained; (iii) an increase in the sulfiding temperature from 500 to 600 °C does not improve considerably the catalytic activity; (iv) the influence of the cesium precursor salt reveals that in spite of the same dispersion of the active phase, the usage of cesium hydroxide improves the amount of labile sulfur/the number of CUS sites and decreases the deactivation by coke.

AUTHOR INFORMATION

Corresponding Author

*Phone: (+34) 952131873. Fax: (+34) 952137534. E-mail: castellon@uma.es (E.R.-C.), ainfantes@icp.csic.es (A.I.-M.).

Funding Sources

We gratefully acknowledge the support from the Ministry of Science and Innovation, Spain (MICINN, España) through the project MAT2009-10481, the Regional Government (JA) through the Excellence Projects (P06-FQM-01661 and P07-FQM-5070) and FEDER funds. A.R.P. thanks the CONACyT (México) for its financial support (Scholarship No. 189933). A.I.M. also thanks the MICINN, Spain, for a Juan de la Cierva contract.

REFERENCES

(1) Hsu, C. S.; Robinson, P. R. *Practical Advances in Petroleum Processing*; Springer: New York, 2006; Vol. 1.
(2) http://www.dieselnet.com/standards/eu/ld.php.
(3) Pecoraro, T. A.; Chianelli, R. R. *J. Catal.* **1981**, *67*, 430–445.
(4) Toulhoat, H.; Raybaud, P.; Kasztelan, S.; Kresse, G.; Hafner, J. *Catal. Today.* **1999**, *50*, 629–636.
(5) De los Reyes, J. A. *Appl. Catal., A* **2007**, *322*, 106–112.
(6) Ledoux, M. J.; Michaux, O.; Agostini, G. *J. Catal.* **1986**, *102*, 275–288.
(7) De los Reyes, J. A.; Göbölös, S.; Vrinat, M.; Breysse, M. *Catal. Lett.* **1990**, *5*, 17–24.
(8) Kuo, Y. J.; Cocco, R. A.; Tatarchuk, B. J. *J. Catal.* **1988**, *112*, 250–266.
(9) Liaw, S. J.; Lin, R.; Raje, A. P.; Davis, B. H. *Appl. Catal., A* **1997**, *151*, 423–435.
(10) De los Reyes, J. A.; Vrinat, M.; Geantet, C.; Breysse, M.; Grimblot, J. *J. Catal.* **1993**, *142*, 455–464.
(11) Scott, C. E.; Betancourt, P.; M. Pérez Zurita, J.; Bolívar, C.; Goldwasser, J. *Appl. Catal., A* **2000**, *197*, 23–29.
(12) Pawelec, B.; Navarro, R. M.; Campos-Martin, J. M.; López Agudo, A.; Vasudevan, P. T.; Fierro, J. L. G. *Catal. Today.* **2003**, *86*, 73–85.
(13) Cattenot, M.; Geantet, C.; Glasson, C.; Breysse, M. *Appl. Catal., A* **2001**, *213*, 217–224.
(14) Pawelec, B.; Navarro, R. M.; Castaño, P.; Álvarez-Galván, M. C.; Fierro, J. L. G. *Energy Fuels* **2009**, *23*, 1364–1372.
(15) Lee, D. K.; Lee, I. C.; Woob, S. I. *Appl. Catal., A* **1994**, *109*, 195–210.
(16) Raje, A. P.; Liaw, S. J.; Davis, B. H. *Appl. Catal., A* **1997**, *151*, 319–342.
(17) Raje, A. P.; Liaw, S. J.; Srinivasan, R.; Davis, B. H. *Appl. Catal., A* **1997**, *150*, 297–318.
(18) Quartararo, J.; Mignard, S.; Kasztelan, S. *J. Catal.* **2000**, *192*, 307–315.
(19) De Los Reyes, J. A.; Vrinat, M.; Geantet, C.; Breysse, M. *Catal. Today* **1991**, *10*, 645–664.
(20) Ishihara, A.; Nomura, M.; Kabe, T. *Chem. Lett.* **1992**, *12*, 2285–2288.
(21) Ishihara, A.; Lee, J.; Dumeignil, F.; Wang, A.; Qian, E. W.; Kabe, T. *J. Catal.* **2003**, *217*, 59–68.
(22) Ishihara, A.; Lee, J.; Dumeignil, F.; Yamaguchi, M.; Hirao, S.; Qian, E. W.; Kabe, T. *J. Catal.* **2004**, *224*, 243–251.
(23) Ishihara, A.; Yamaguchi, M.; Godo, H.; Qian, W.; Godo, M.; Kabe, T. *Chem. Lett.* **1996**, *25*, 743–744.
(24) Romero-Pérez, A.; Infantes-Molina, A.; Rodríguez-Castellón, E.; Jiménez-López, A. *Appl. Catal., B* **2010**, *97*, 257–268.
(25) Gómez-Cazalilla, M.; Mérida-Robles., J. M.; Gurbani, A.; Rodríguez Castellón, E.; Jiménez-López, A. *J. Solid State Chem.* **2007**, *180*, 1130–1140.
(26) Castillo-Villalón, P.; Ramírez, J.; Maugé., F. *J. Catal.* **2008**, *260*, 65–74.
(27) Berhault, G.; Lacroix, M.; Breysse, M.; Maugé, F.; Lavalley, J. C.; Nie, H.; Qu, L. *J. Catal.* **1998**, *178*, 555–565.
(28) Moulder, J. F.; Stickle, W. F.; Sobol, P. E.; Bomben, K. D. *Handbook of X-ray Photoelectron Spectroscop*; Chastain, J., Ed.; Perkin-Elmer: Eden Prairie, MN, 1992.

(29) http://www.lasurface.com.
(30) Rodriguez, J. A.; Jirsak, T.; Chaturvedi, S.; Hrbek, J. *Surf. Sci.* **1998**, *407*, 171–188.
(31) Mazzieri, V.; Coloma-Pascual, F.; Arcoya, A.; L'Argentière, P. C.; Fígoli., N. S. *Appl. Surf. Sci.* **2003**, *210*, 222–230.
(32) Braos-García, P.; García-Sancho, C.; Infantes-Molina, A.; Rodríguez-Castellón, E.; Jiménez-López, A. *Appl. Catal., A* **2010**, *381*, 132–144.
(33) Geantet, C.; Gobölös, S.; De Los Reyes, J. A.; Cattenot, M.; Vrinat, M.; Breysse., M. *Catal. Today* **1991**, *10*, 665–680.
(34) Berhault, G.; Lacroix, M.; Breysse, M.; Maugé, F.; Lavalley, J. C.; Lu, L. L. *J. Catal.* **1997**, *170*, 37–45.
(35) Mangnus, P. J.; Riezebos, A.; van Langeveld, A. D.; Moulijn., A. *J. Catal.* **1995**, *151*, 178–191.
(36) Labruyère, F.; Lacroix, M.; Schweich, D.; Breysse., M. *J. Catal.* **1997**, *167*, 464–469.
(37) Knudsen, K. G.; Cooper, B. H.; Topsøe, H. *Appl. Catal, A* **1999**, *189*, 205–215.
(38) Dumonteil, C.; Lacroix, M.; Geantet, C.; Jobic, H.; Breysse., M. *J. Catal.* **1999**, *187*, 464–473.
(39) Lacroix, M.; Midoratos, C.; Breysse, M.; Decamp, T.; Yuan, S.; Solymosi, F.; Tétànyi., P.; Guezi., L. *New Frontiers in Catalysis*; Elsevier: Budapest, Hungary, 1993.
(40) Ishihara, A.; Godo, H.; Kanamori, R.; Qian, W.; Kabe, T. *Appl. Catal., A* **1999**, *182*, 345–355.
(41) Ishihara, A.; Nomura, M.; Takahama, N.; Hamaguchi, K.; Kabe, T. *Sekiyu Gakkaishi.* **1996**, *39*, 211–221.
(42) Ishihara, A.; Yamaguchi, M.; Godo, H.; Qian, W.; Godo, M.; Kabe, T. *Sekiyu Gakkaishi.* **1998**, *41* (1), 51–58.
(43) Dinerman, C. E.; Ewing, G. E. *J. Phys. Phys.* **1970**, *53*, 626–632.